ELEMENTA
Science of the Anthropocene

Seasonal phytoplankton blooms in the North Atlantic linked to the overwintering strategies of copepods

Kevin D. Friedland[1*] • Nicholas R. Record[2] • Rebecca G. Asch[3] • Trond Kristiansen[4] • Vincent S. Saba[5] • Kenneth F. Drinkwater[4] • Stephanie Henson[6] • Robert T. Leaf[7] • Ryan E. Morse[1] • David G. Johns[8] • Scott I. Large[9] • Solfrid S. Hjøllo[4] • Janet A. Nye[10] • Mike A. Alexander[11] • Rubao Ji[12]

[1]National Marine Fisheries Service, Narragansett, Rhode Island, United States
[2]Bigelow Laboratory for Ocean Sciences, East Boothbay, Maine, United States
[3]Princeton University, Program in Atmospheric and Oceanic Sciences, Princeton, New Jersey, United States
[4]Institute of Marine Research, Nordnes, Bergen, Norway
[5]National Marine Fisheries Service, Northeast Fisheries Science Center, c/o NOAA Geophysical Fluid Dynamics Laboratory, Princeton University Forrestal Campus, Princeton, New Jersey, United States
[6]National Oceanography Centre, European Way, Southampton, United Kingdom
[7]Gulf Coast Research Laboratory, University of Southern Mississippi, Ocean Springs, Mississippi, United States
[8]Sir Alister Hardy Foundation for Ocean Sciences, Citadel Hill, Plymouth, United Kingdom
[9]ICES, Copenhagen, Denmark
[10]School of Marine and Atmospheric Sciences, Stony Brook University, Stony Brook, New York, United States
[11]NOAA, Earth System Research Laboratory, Boulder, Colorado, United States
[12]Department of Biology, Woods Hole Oceanographic Institution, Woods Hole, Massachusetts, United States
*kevin.friedland@noaa.gov

Abstract

The North Atlantic Ocean contains diverse patterns of seasonal phytoplankton blooms with distinct internal dynamics. We analyzed blooms using remotely-sensed chlorophyll *a* concentration data and change point statistics. The first bloom of the year began during spring at low latitudes and later in summer at higher latitudes. In regions where spring blooms occurred at high frequency (i.e., proportion of years that a bloom was detected), there was a negative correlation between bloom timing and duration, indicating that early blooms last longer. In much of the Northeast Atlantic, bloom development extended over multiple seasons resulting in peak chlorophyll concentrations in summer. Spring bloom start day was found to be positively correlated with a spring phenology index and showed both positive and negative correlations to sea surface temperature and the North Atlantic Oscillation in different regions. Based on the characteristics of spring and summer blooms, the North Atlantic can be classified into two regions: a seasonal bloom region, with a well-defined bloom limited to a single season; and a multi-seasonal bloom region, with blooms extending over multiple seasons. These regions differed in the correlation between bloom start and duration with only the seasonal bloom region showing a significant, negative correlation. We tested the hypothesis that the near-surface springtime distribution of copepods that undergo diapause (*Calanus finmarchicus*, *C. helgolandicus*, *C. glacialis*, and *C. hyperboreus*) may contribute to the contrast in bloom development between the two regions. Peak near-surface spring abundance of the late stages of these *Calanoid* copepods was generally associated with areas having a well-defined seasonal bloom, implying a link between bloom shape and their abundance. We suggest that either grazing is a factor in shaping the seasonal bloom or bloom shape determines whether a habitat is conducive to diapause, while recognizing that both factors can re-enforce each other.

Domain Editor-in-Chief
Jody W. Deming, University of Washington

Associate Editor
Julie E. Keister, University of Washington

Knowledge Domains
Ocean Science
Earth & Environmental Science
Ecology

Article Type
Research Article

Part of an *Elementa* Special Feature
Climate change impacts: Fish, fisheries and fisheries management

Received: September 13, 2015
Accepted: March 8, 2016
Published: April 7, 2016

Introduction

In the North Atlantic, the timing of the onset of phytoplankton blooms can vary between years by as much as a month in the subtropics and subpolar gyre and by 2–3 months in the transition zone between gyres (Henson et al., 2009). Extensive oceanographic research has examined the bio-physical factors associated with the variable timing of bloom onset. Key hypotheses formulated to explain the timing of the spring bloom in temperate-to-polar regions include: (1) Sverdrup's critical depth hypothesis, which asserts that blooms occur when seasonal light limitation eases due to the shoaling of the mixed layer above a critical depth, where depth-integrated phytoplankton growth through photosynthesis and losses due to respiration and grazing are equal (Sverdrup, 1953); (2) the critical turbulence hypothesis, which states that blooms begin when turbulent mixing of the upper water column weakens enough for phytoplankton to accumulate in the euphotic zone (Huisman et al., 1999; Taylor and Ferrari, 2011), where the decrease in turbulence may occur before the mixed layer depth shoals; and (3) the Dilution–Recoupling Hypothesis, which posits that the onset of positive phytoplankton growth is associated with a deepening of the mixed layer that "disturbs" the balance between phytoplankton and grazers by diluting the prey field and reducing predator-prey encounter rates (Behrenfeld, 2010). Recently, Chiswell et al. (2015) suggested that these three hypotheses can be unified into one model, as they are likely to operate at different times of the year and in different areas of the water column.

The phytoplankton blooms of the North Atlantic, and in particular the spring bloom, have been studied extensively from a biogeographical perspective. The distribution of bloom patterns is well understood; however, studies of the biogeography of blooms emphasize different nuances of the ecology of blooms depending on the nature of the models and analysis used. Patterns of bloom timing have been found to be related to oceanic provinces associated with latitudinal patterns of atmospherically driven mixing (Follows and Dutkiewicz, 2002); mixing was associated with North Atlantic Oscillation phase resulting in regional differences in the start of the spring bloom. Martinez et al. (2011) studied North Atlantic bloom patterns to better understand the relationship between the development of water column stratification and the onset of blooms. Their data challenged the common conception that increased stratification limits nutrient supply and thus results in reduced primary production, which is expected to dominate over the potential for warmer temperature to increase metabolic rates and thus increase primary production. D'Ortenzio et al. (2012) analyzed regimes in bloom phenology in remote sensing data, providing a global classification of these regimes. Vargas et al. (2009) and Sapiano et al. (2012) also studied bloom phenology by fitting generalized linear models to the data. Taboada and Anadon (2014) examined trends in bloom phenology in the North Atlantic and found wind forcing exerted dominant control over bloom timing, though local temperature and insolation may play important roles. Lacour et al. (2015) analyzed bloom cycles in the North Atlantic subpolar gyre and identified bioregions with cluster analysis. These bioregions reflected differing patterns of bloom initiation and duration; furthermore, they suggest that blooms are initiated by light and mixing conditions since nutrients are not limiting locally, and that blooms terminate in response to top-down grazing pressures. As comprehensive as the body of literature on the biogeography of North Atlantic blooms appears, there are still aspects of bloom development that require further study.

Comparatively little research has investigated the consequences of interannual variation in bloom timing. Such interannual variability has the potential to influence the development of the bloom, coupling between primary and secondary production, and fluxes of organic matter to the benthos. In particular, the relationship between bloom timing, duration, and magnitude has not been previously investigated in detail, although a few studies have briefly noted a linkage between these bloom characteristics. Early blooms may be especially long lived due to the fact that they tend to occur in colder water, which is associated with slower rates of phytoplankton growth (Song et al., 2011), and because these blooms are less likely to be grazed by mesozooplankton prior to their seasonal emergence from diapause. Racault et al. (2012) reported a negative correlation between bloom timing and duration, with early bloom onset associated with longer blooms in several ocean basins. A similar pattern was observed by Friedland et al. (2015) in the Gulf of Maine and along the shelf break of the east coast of North America. Evidence for a relationship between bloom timing and magnitude is mixed, with significant correlations between these bloom characteristics identified in some regions, but not others (Henson et al., 2009; Henson and Thomas, 2007; Song et al., 2011).

The role of zooplankton in shaping the time course development of a bloom is also complex, and direct lines of causation are not well understood. Micro- and mesozooplankton communities are diverse, representing a variety of feeding strategies and diets. Because of the rapid doubling rates of microzooplankton, this group has more of a direct control on phytoplankton loss rates than mesozooplankton grazing, with microzooplankton grazing accounting for the majority of phytoplankton losses (Banse, 2013; Chen et al., 2013; Landry and Calbet, 2004; Verity et al., 1993). Mesozooplankton can have a significant impact on microzooplankton via predation, which can in turn disrupt the balance between gain and loss of phytoplankton abundances, producing rapid changes in bloom dynamics (Behrenfeld and Boss, 2014). The role of zooplankton in shaping phytoplankton blooms has often been underappreciated (Banse, 2013). Because of complex multi-trophic interactions (Behrenfeld and Boss, 2014), uncertainties associated with direct measurement of *in situ* grazing

rates (Kiørboe et al., 1985), and synergistic effects with other sources of mortality, such as viral lysis (Bidle and Vardi, 2011; Suttle et al., 1990) and programmed cell death (Bidle and Falkowski, 2004), quantifying the role of grazing in shaping phytoplankton blooms is a challenge that requires multiple lines of evidence.

Here we describe and analyze seasonal phytoplankton blooms in the North Atlantic as defined as events detected using change point statistics (Friedland et al., 2015) as opposed to other frequently used algorithms which generally rely on threshold methods and curve fitting (Blondeau-Patissier et al., 2014; Brody et al., 2013; Ueyama and Monger, 2005). The change point approach provides distinct determinations of bloom start and end, which allows exploration into the internal dynamics of blooms including the relationships between bloom start and measures of bloom size. The search for blooms was structured to bracket multiple seasons to account for North Atlantic blooms that occur from spring into fall. We then turned our attention to the potential role of zooplankton in shaping the spatial pattern of spring and summer blooms. We also compared the distribution of size and functional groups of zooplankton to the patterns of bloom shape and dynamics.

Methods

Spatial extent of analyses

We analyzed phytoplankton blooms, sea surface temperature, and zooplankton abundance over the geographic extent of the North Atlantic from 100°W to 30°E and from 20 to 70°N (Figure 1). Chlorophyll concentrations were extracted from remote sensing databases using a grid of 1° squares centered on half degrees. These extractions yielded bloom data for 4,263 grid locations, some of which were located in inland waters and thus not of primary interest. Sea surface temperatures were extracted for the same grid used for the chlorophyll data yielding 4,155 SST grid locations; the lesser number of locations reflects different assumptions used for land masking in the two databases. The extent of this grid was not shown in Figure 1 since it essentially covers all open water areas. Zooplankton data were also analyzed on a 1° grid, but the grid locations were centered on whole degrees and for a limited spatial extent as shown in Figure 1. Finally, three index areas were used to characterize annual chlorophyll concentration patterns associated with regional differences in bloom timing and frequency (Figure 1).

Seasonal plankton bloom analyses

Chlorophyll *a* concentrations were based on remote-sensing measurements made with the Sea-viewing Wide Field of View (SeaWiFS) and Moderate Resolution Imaging Spectroradiometer (MODIS), Medium Resolution Imaging Spectrometer (MERIS), and Visible and Infrared Imager/Radiometer Suite (VIIRS) sensors. We used the GSM (Garver, Siegel, Maritorena Model) merged data product at 100 km and 8-day spatial and temporal resolutions, respectively, obtained from the Hermes GlobColour website (http://hermes.acri.fr/index.php). These four sensors provide an overlapping time series of chlorophyll *a* concentrations during the period 1998 to 2014 and were combined based on a bio-optical model inversion algorithm (Maritorena et al., 2010).

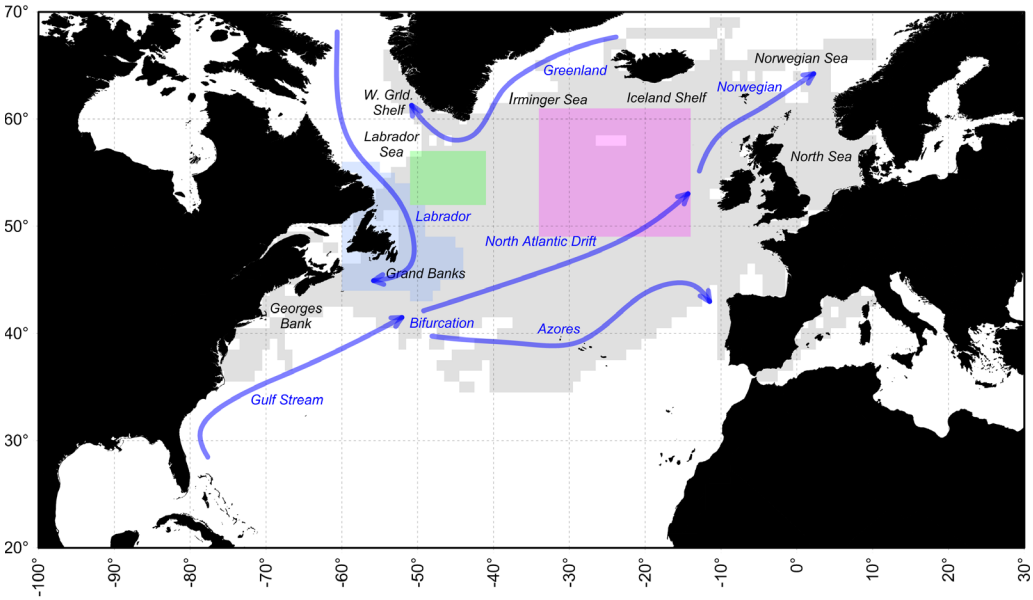

Figure 1

Study area and bloom index areas.

Study area for chlorophyll, sea surface temperature, and zooplankton analyses. Three index areas (spring high frequency, summer high frequency, and summer low frequency areas, shown in blue, green, and magenta, respectively) were used to characterize annual chlorophyll patterns. Area shaded gray (including areas overlapping index areas) is the spatial extent of zooplankton samples. North Atlantic currents shown as blue arrows.

doi: 10.12952/journal.elementa.000099.f001

Table 1. Bloom search parameters and blooms detected by latitudinal bands

Latitude band	Search start day[a]			Patterns evaluated[b]			Blooms detected		
	Spring	Summer	Fall	Spring	Summer	Fall	Spring	Summer	Fall
65 – 69	65	97	—	4,468	5,024	—	2,684	2,350	—
60 – 64	49	97	—	5,965	7,494	—	2,761	2,904	—
55 – 59	33	97	—	6,405	7,792	—	2,994	3,645	—
50 – 54	17	97	169	5,087	5,670	5,411	2,439	2,617	1,341
45 – 49	1	97	185	5,783	5,984	5,875	2,765	1,908	1,609
40 – 44	1	97	185	7,457	7,532	7,515	4,652	874	1,921
35 – 39	1	97	185	8,299	8,319	8,327	4,315	261	671
30 – 34	1	97	185	7,464	7,476	7,473	2,183	384	226
25 – 29	1	97	185	7,165	7,161	7,163	811	920	413
20 – 24	1	97	185	6,919	6,837	6,889	639	1,364	900
Total				65,012	69,289	48,653	26,243	17,227	7,081

[a]Search start day is first day of the half year (23 8-day periods) time series used to search for spring, summer, and fall blooms.
[b]Patterns or time series were evaluated over the period 1998–2014.
doi: 10.12952/journal.elementa.000099.t001

Phytoplankton blooms, as evidenced by changes in chlorophyll concentration, were detected in three overlapping seasons in the North Atlantic using a bloom detection algorithm designed to find bloom start and end points. The algorithm searches for a single bloom event occurring within a time series of 23 8-day chlorophyll concentration composites (i.e., over a half-year period). Recognizing that more than one bloom can occur during the year, three seasonal time frames were examined for blooms, the temporal extents of which varied by latitude. As explained in detail in the methods description of the bloom detection algorithm, we wanted to detect seasonal blooms of limited duration and therefore did not try to describe multi-season increases in chlorophyll concentration lasting longer than three months. The first seasonal time frame of the year detected spring blooms in time series starting from day 1 (January 1) over a range of latitudes of 20–49°N (Table 1). The time series used in the spring bloom analysis shifted to progressively later in the year to day 65 (March 5) above 65°N to conform to the availability of usable remote sensing data at higher latitudes. Over the study period of 1998–2014, spring bloom detections were conducted on a potential 65,012 spring chlorophyll time series patterns. The search for summer period blooms started at the same time over all latitudes, day 97 (April 4), and was conducted for 69,289 patterns. The search for fall blooms started on day 185 (July 3) and shifted to earlier in the year with latitude until the overlap with the period used to search for summer blooms increased to the point making a separate search for fall blooms meaningless. In total, seasonal bloom detections were conducted on 182,954 time series patterns.

We identified the beginning and end of seasonal blooms in each chlorophyll concentration time series using change-point analysis. The sequential averaging algorithm called STARS or "sequential *t*-test analysis of regime shifts" (Rodionov, 2004, 2006) was used to find all change points in a time series. STARS algorithm parameters were specified *a priori*: the alpha level used to test for a change in the mean was set to $\alpha = 0.1$; the length criteria, the number of time steps to use when calculating the mean level of a new regime, was set to 5; and, the Huber weight parameter, which determines the relative weighting of outliers in the calculation of the regime mean, was set to 3. A bloom was considered to have occurred if there was a period bracketed by a positive and negative change-point. We ignored change-points (positive or negative) that occurred in the first or last two periods of the time series (8-day periods 1, 2, 22 and 23). A detected bloom could not exceed nine sample periods (approximately 2.4 months), which was based on analyses of climatological bloom patterns in the Northwest Atlantic (Friedland and Todd, 2012). The minimum duration of a bloom was three sample periods, which represents the minimum span the algorithm needed to find a positive followed by a negative change-point. Periods bracketed by positive and negative change-points exceeding nine 8-day periods were considered to be ecologically different from discrete seasonal blooms. This method has been used in previous analyses of Northeast Shelf bloom patterns (Friedland et al., 2008, 2009) and of Northwest Atlantic Arctic and Subarctic patterns (Friedland and Todd, 2012).

We extracted statistics to characterize the timing and attributes of each bloom event. Also, for each location and season, we calculated a bloom frequency as the proportion of the study years in which a bloom was detected. Bloom start was defined as the first day of the year of the bloom period. Bloom intensity was the average of the chlorophyll concentrations during the bloom period. Bloom magnitude was the integral of the chlorophyll concentrations during the bloom period. Magnitude can be calculated as the sum of the chlorophyll concentrations during the blooms, which carries the unit mg m^{-3}; or, as the product of the mean chlorophyll concentration during the bloom and the duration in 8-day periods, which carries the unit

mg m^{-3} 8-day. We used to the later unit designation to distinguish it from bloom intensity. For each grid location of the three seasonal time frame analyses, we examined the correlation between bloom start and intensity, duration, and magnitude. These correlations were limited to locations with a minimum of eight detected blooms.

Bloom shape parameter

Guided by the average annual pattern of chlorophyll concentration for the three index areas, we developed a bloom shape parameter. For grid locations within the three index areas (Figure 1), we computed mean chlorophyll concentrations by day of the year. For these same areas, we also computed normalized (Z-scores) chlorophyll concentration and centered each time series on the date of occurrence of the maximum chlorophyll concentration. The bloom shape parameter, computed for study grid locations where there were at least eight years with spring or summer blooms, was expressed as the coefficient of variation (C_V) of the chlorophyll concentrations during the eleven 8-day periods bracketing the maximum chlorophyll concentration of the bloom. Areas with low C_V were characterized by blooms that often extended beyond the limits of the detection algorithm and were essentially multi-season in length. Regions with a high C_V pattern were more likely to have short duration, intense blooms that were detected by our algorithm and occurred within a single season. The bloom shape parameter was plotted with average April SST based on the temperature data described below.

Forcing related to the initiation of spring blooms

The effect of seasonally warmer ocean conditions on the timing of the spring bloom was tested using an index of spring thermal phenology and the SST associated with the bloom start day. The phenology index was based on the date the average annual temperature for a specific location, the transition temperature, was exceeded within a given year (Friedland et al., 2015). The dataset used in the analysis was the NOAA Optimum Interpolation ¼ Degree Daily Sea Surface Temperature Analysis (OISST) dataset, which provides high resolution SST with a spatial grid resolution of 0.25° and temporal resolution of 1 day (Reynolds et al., 2007). For each year and grid location, the daily temperature data were smoothed with a 5-point moving average filter; the first day of the year that exceeded the transition temperature was scored as the spring transition date. The search for spring transition dates was constrained to a 90-day period (April 14 to July 13). If the transition temperature was not detected in a period it was scored as a missing data value. The SST associated with the bloom start day was also extracted from the OISST dataset by sampling the proximate grid location and day associated with each bloom start. For each grid location, we examined the correlation between spring bloom start day and spring thermal transition date and associated SST over the time series. These correlations were limited to locations with at least eight years with detected blooms.

The effect of the North Atlantic Oscillation (NAO) on the start of the spring bloom was tested using the NAO winter index. The NAO is defined as the difference in normalized sea level pressure (SLP) between Lisbon, Portugal, and Stykkishólmur, Iceland; the winter index is averaged over December through March (Hurrell et al., 2001). For each grid location, we examined the correlation between the spring bloom start day and the NAO index. These correlations were limited to locations with at least eight years with detected blooms.

North Atlantic zooplankton

The abundances of copepods that graze on phytoplankton blooms were extracted from the Continuous Plankton Recorder (CPR) database hosted by the Sir Alister Hardy Foundation for Ocean Science (SAHFOS, http://www.sahfos.ac.uk/). The CPR samples near-surface waters (~ 10 m depth) from ships of opportunity. The database contains ~ 200,000 samples and provides spatial and temporal representations of zooplankton distributions that compare well with other sampling gears (Hélaouët et al., 2016). We examined the spatial abundances of small and large copepods from the CPR samples. Small copepod counts were from the traverse stage of the CPR analysis, which included specimens seen in a subsample that were ≤ 2 mm including small species and juvenile forms, such as *Calanus* stages I–IV. The traverse stage of the analysis was made with 54x magnification, directly from the silk mesh sampling material. Large copepod counts were of specimens > 2 mm taken from the eyecount stage of the CPR analysis. The eyecount stage of the analysis entails visually counting all larger copepods removed from the silk (Richardson et al., 2006). We also examined the spatial abundance of four copepod species that diapause in the North Atlantic, *Calanus finmarchicus*, *C. helgolandicus*, *C. glacialis*, and *C. hyperboreus*: the first three taxa include stage V copepodites and adults (CV–CVI), while the *C. hyperboreus* taxon includes stages CIII–CVI. Although *C. helgolandicus* has an abbreviated active dormancy (Wilson et al., 2015), we included it because it is a significant phytoplankton grazer and lipid accumulator. Because these species undergo diapause and are out of the CPR sampling depth during winter, we used spring abundances. April through July abundances were gridded to a 1° grid (described above) for the period 1958–2014; the abundances were plotted on a log scale. To evaluate the relationship between bloom shape and the distribution of the full range of copepod taxa, the total abundances of small and large copepods were

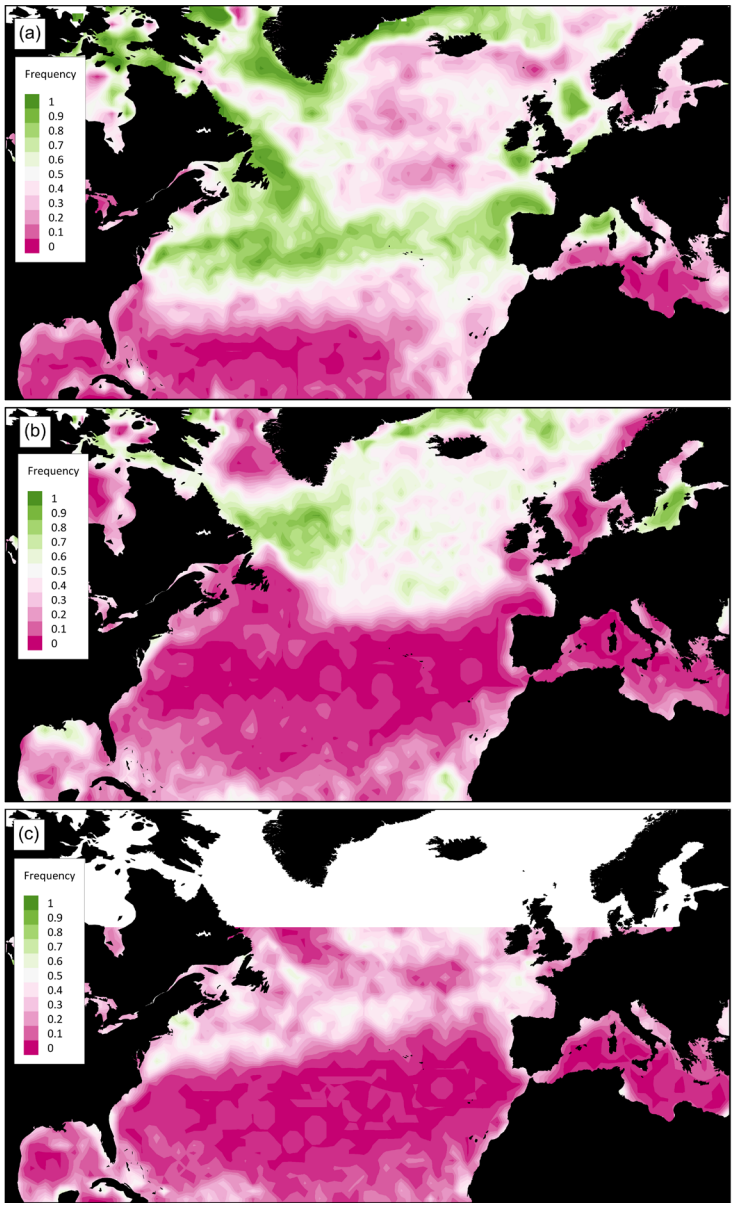

Figure 2
North Atlantic bloom frequency.

Spring (a), summer (b), and fall (c) bloom frequencies defined as the ratio of years with blooms divided by the total number of years over the period 1998–2014.

doi: 10.12952/journal.elementa.000099.f002

plotted over the study area. To explore the relationship between bloom shape and the presence of copepods that undergo diapause, the peak abundances of the four *Calanoid* taxa listed above were overlaid on the area of low C_V bloom shape parameter.

Results

Seasonal bloom dynamics

The frequency of seasonal blooms showed distinct geographic patterns across the North Atlantic basin. Spring bloom frequency was highest north of the 35°N meridian with the exception of a portion of the Northeast Atlantic associated with the Irminger and Iceland basins south to the 50°N meridian and parts of the Labrador and Norwegian seas (Figure 2a). Spring bloom frequency on the Newfoundland-Labrador, Scotian and Northeast US shelves was generally 0.9, indicating that a spring bloom was detectable in most years. Spring bloom frequency in the Northeast Atlantic was low, but generally did not reach zero frequency, thus spring blooms occurred in these areas in some years. The most southern latitude bands for the study area had locations with spring bloom frequencies of zero. The pattern of summer bloom frequency was complimentary to the spring bloom pattern with summer blooms most frequently detected in the Labrador Sea and the Northeast Atlantic areas that had a low spring bloom frequency (Figure 2b). Some summer blooms were detected at the low latitude bands of the study area as well. Fall blooms in the study area were restricted to a

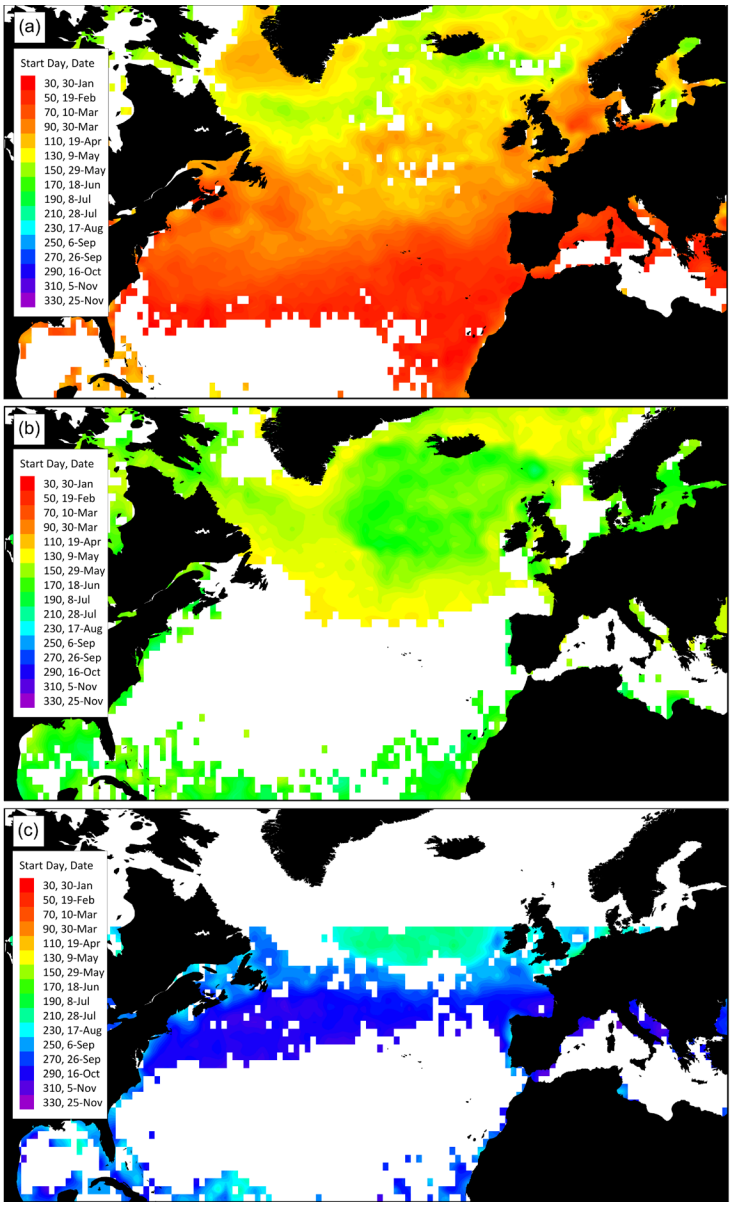

Figure 3
North Atlantic bloom start day.

Spring (a), summer (b), and fall (c) bloom start day and date over the period 1998–2014. Only grid locations with at least three years with detected blooms were included in plot.

doi: 10.12952/journal.elementa.000099.f003

band extending from the continental shelves of the Northeast US north to Newfoundland-Labrador across the Atlantic basin to the Celtic-Biscay Shelf (Figure 2c). The location of this band approximately coincided with the transition zone between the North Atlantic subtropical and subpolar gyres. Fall bloom frequencies were at high levels in isolated pockets in this area.

Bloom start dates varied between and within seasons. Spring blooms started at the end of March into the beginning of April on the Newfoundland-Labrador, Scotian and Northeast US shelves (Figure 3a). The spring blooms in the Labrador Sea started a few weeks later in mid-April and later still in the Norwegian Sea in the beginning of May. Summer blooms in the Labrador Sea tended to start in the beginning of June (Figure 3b), whereas the summer blooms in the Northeast Atlantic associated with the Irminger and Iceland basins started in the beginning of July (Figure 3b). Fall bloom start dates were highly variable, though most tended to start by the beginning of October (Figure 3c). Blooms found in the fall bloom search that started around day 170 (late June) were likely from the same grouping of blooms that were detected in the summer bloom search.

Bloom magnitude was highest for blooms occurring on shelf seas and lowest in mid-ocean basin areas, especially in the south of the study domain. Spring bloom magnitudes reached levels around 20 mg m^{-3} 8-day in both the eastern and western margins of the ocean basin (Figure 4a). The highest magnitude blooms were found on Georges Bank, Grand Banks, West Greenland Shelf, Iceland Shelf, and the North and Norwegian Seas. Spring bloom magnitudes were on the order of 5 mg m^{-3} 8-day in many mid-ocean areas. In areas where

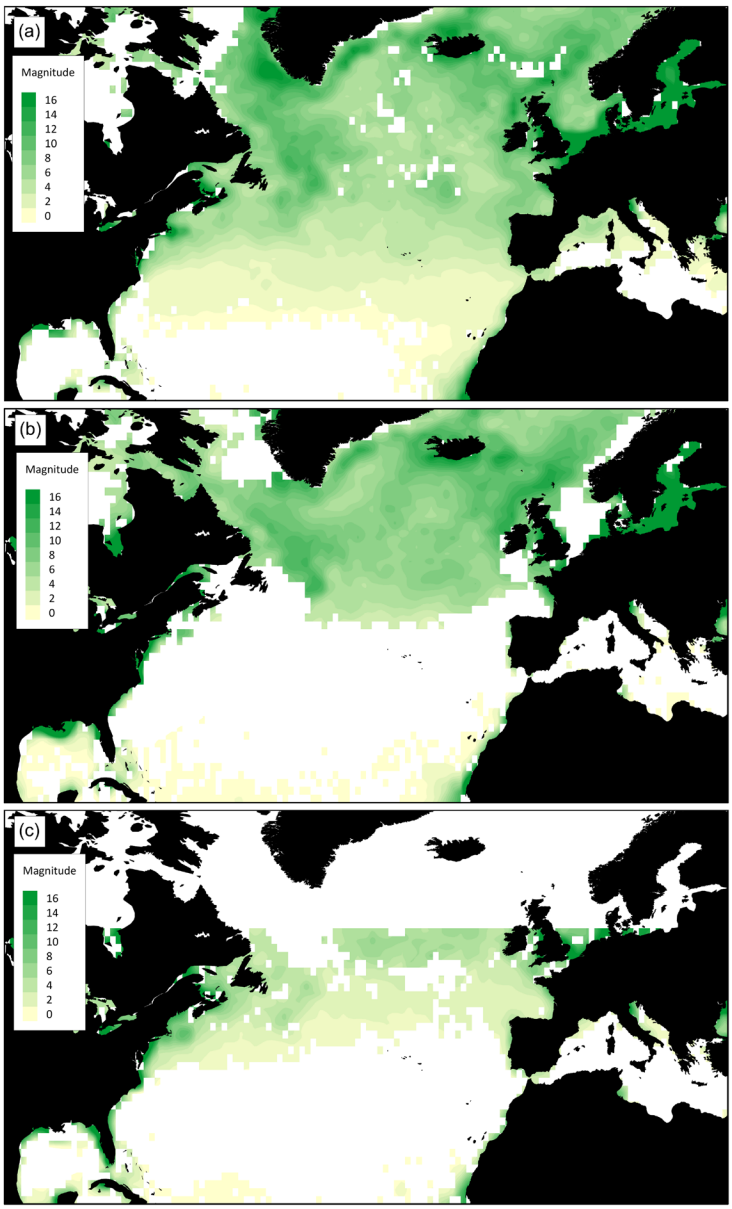

Figure 4

North Atlantic bloom magnitude.

Spring (a), summer (b), and fall (c) bloom magnitudes (mg m^{-3} 8-day) over the period 1998–2014. Only grid locations with at least three years with detected blooms were included in plot.

doi: 10.12952/journal.elementa.000099.f004

summer blooms occurred at high frequency, such as the Labrador Sea and the Northeast Atlantic, bloom magnitudes tended to be smaller than typical spring bloom magnitudes, ranging from 5 to 10 mg m^{-3} 8-day (Figure 4b). Fall blooms in the band extending from the continental shelves of the Northeast US north to Newfoundland-Labrador across the Atlantic basin to the Celtic-Biscay Shelf also tended to be smaller than spring blooms, with magnitudes ranging from 5 to 10 mg m^{-3} 8-day (Figure 4b).

Relationships between bloom start day and bloom parameters

The timing of the spring bloom was more highly correlated with bloom duration and bloom magnitude than bloom intensity. Bloom intensity was weakly correlated with bloom start day with a mixed correlation field of both positive and negative correlations, though the correlations were more positive in sub-polar latitudes (Figure 5a). On the other hand, bloom duration was strongly correlated with bloom start day and the correlations were exclusively negative in sign (Figure 5b). These correlations indicate that early blooms were associated with long lasting blooms. Since bloom magnitude was dependent on bloom duration, it is not surprising to see that spring bloom magnitude was also negatively correlated with bloom start day, though the correlations were not as strong as the correlations associated with bloom duration (Figure 5c).

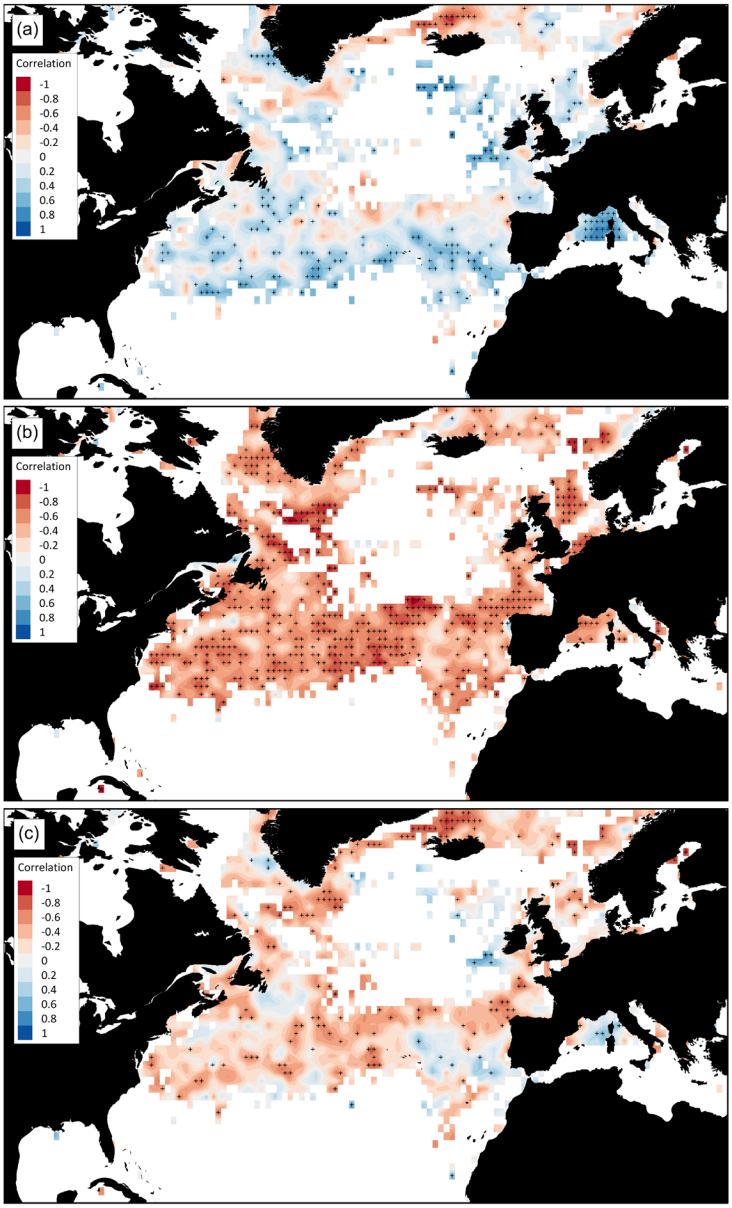

Figure 5

Relationship between spring bloom start day and dimension parameters.

Correlations between start day and spring bloom intensity (a), duration (b), and magnitude (c) for the period 1998–2014. Only grid locations with at least eight years with detected blooms were included; crosses mark locations with significant correlations ($\rho > 0.05$).

doi: 10.12952/journal.elementa.000099.f005

In several regions, the timing of summer blooms was significantly correlated with bloom intensity as well as bloom duration. Bloom intensity was positively correlated with bloom start day in the Irminger Basin area (Figure 6a). The correlation field between bloom start day and duration was comprised of mostly negative correlations, though these correlations were not as strong as in the spring (Figure 6b). The correlation between bloom start day and magnitude reflects the stronger regional correlations between start and intensity or duration: areas where intensity was strongly correlated with start day emerged as areas with positive correlations between start day and bloom magnitude (Figure 6c); and areas where duration was strongly correlated with start day emerged as areas with negative correlations between start day and bloom magnitude.

In the limited range of areas where fall blooms occur, bloom intensity and duration responded differently to bloom timing. Whereas bloom intensity was positively correlated with bloom start day (Figure 7a), bloom duration was negatively correlated with start day (Figure 7b). The stronger of the two correlation fields was the duration field. The bloom magnitude correlations were mostly negative due to the more dominant effect of duration on bloom magnitude as opposed to intensity (Figure 7c).

Forcing related to the initiation of spring blooms

Thermal conditions and basin-scale forcing as indicated by the NAO had distinct regional effects on the initiation of spring blooms. Spring thermal transition day was positively correlated with bloom start day over much of the region where spring blooms occurred in most years (Figure 8a). Only isolated areas had

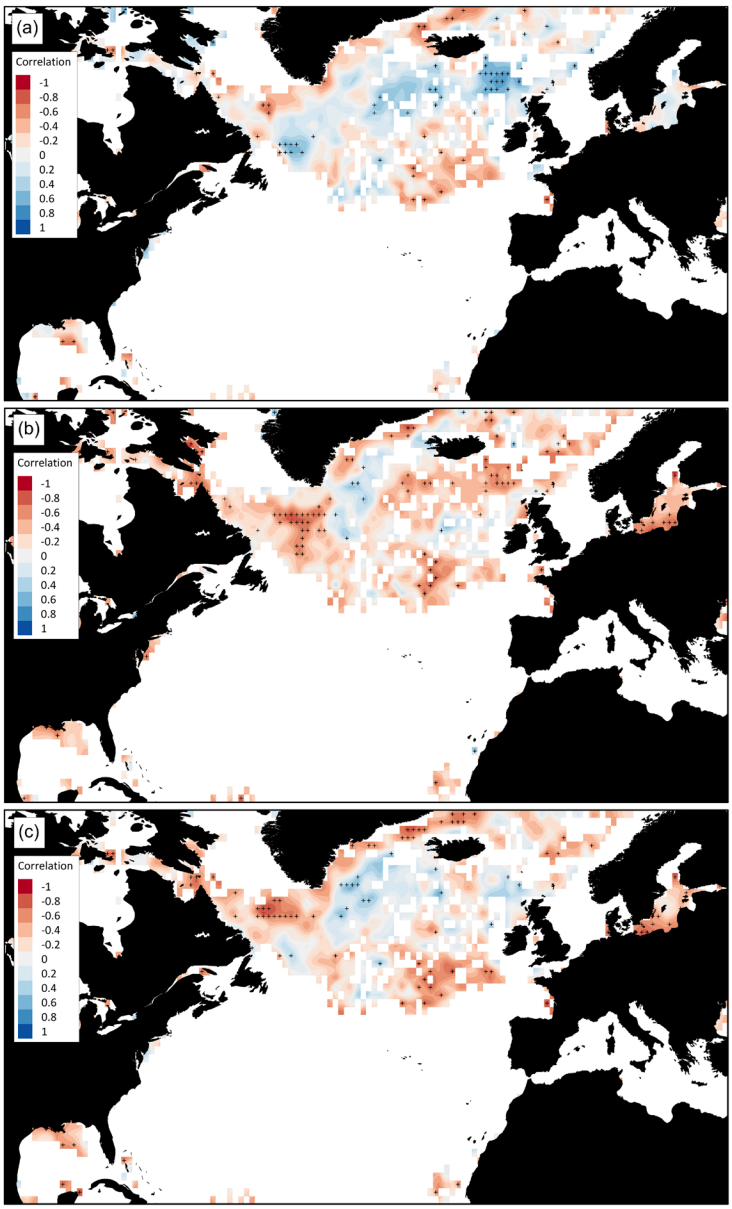

Figure 6

Relationship between summer bloom start day and dimension parameters.

Correlation between start day and summer bloom intensity (a), duration (b), and magnitude (c) for the period 1998–2014. Only grid locations with at least eight years with detected blooms were included; crosses mark locations with significant correlations ($\rho > 0.05$).

doi: 10.12952/journal.elementa.000099.f006

significant negative correlations between transition and start day, specifically along the East Greenland Coast and north of Iceland. SST tended to be positively correlated with bloom start day in northern latitude areas and negatively correlated in southern areas (Figure 8b). The NAO was also correlated with spring bloom timing: the NAO was negatively correlated with the spring bloom at lower latitudes and positively correlated at higher latitudes with the exception of blooms south and east of Greenland (Figure 8c).

Bloom shape parameter

The North Atlantic can be divided into two distinct areas based on the time course shape of chlorophyll concentrations that mark the primary bloom by area. When we examined the average annual pattern of chlorophyll concentration for the three index areas (Figure 1), we found that the areas associated with spring blooms have discrete short duration peaks in chlorophyll associated with the bloom (Figure 9a). The normalized peaks in this area suggest that the duration of the bloom was usually less than the 9 8-day period threshold used on our bloom detection algorithm (Figure 9b). In the index area representing high frequency of summer blooms, we saw a similar pattern. The blooms were discrete and of short duration (Figure 9c), which was reinforced in the normalized data (Figure 9d). In the index area representing summer blooms detected at low frequency, the time-dependent development of chlorophyll concentration was markedly different. Chlorophyll concentration started to increase during spring, did not peak until summer, and remained elevated for a bloom period in excess of five months, well outside the limits of our bloom detection algorithm (Figure 9e).

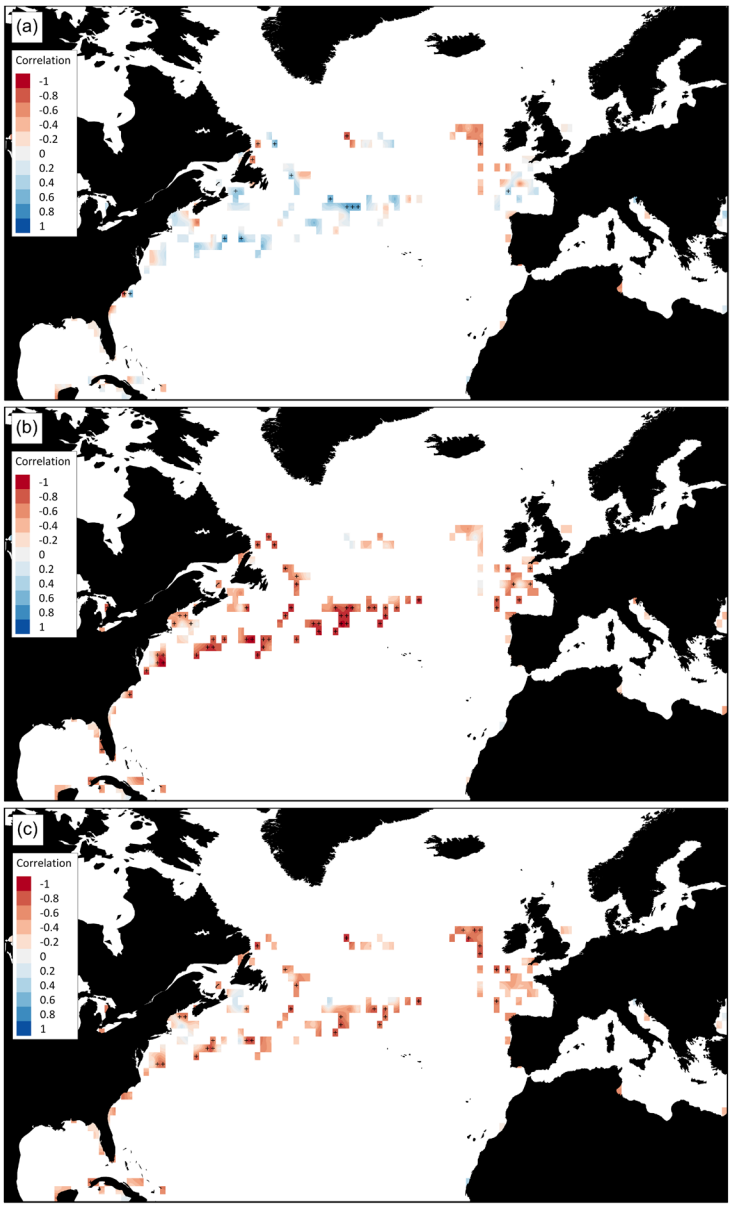

Figure 7

Relationship between fall bloom start day and dimension parameters.

Correlations between start day and fall bloom intensity (a), duration (b), and magnitude (c) for the period 1998–2014. Only grid locations with at least eight years with detected blooms were included; crosses mark locations with significant correlations ($\rho > 0.05$).

doi: 10.12952/journal.elementa.000099.f007

The normalized chlorophyll concentration suggests that the duration of these blooms may be somewhat less than five months (Figure 9f). However the main point is that the shape of the principal annual bloom varies regionally between discrete seasonal blooms where chlorophyll increases and decreases rapidly versus areas where the bloom is a multi-season event with slow rates of increase and decline.

The division of bloom shapes can be visualized on a basin scale using the bloom shape parameter, C_V, which revealed a region in the Northeast Atlantic with low parameter values surrounded by areas with higher values (Figure 10). There was also a small area of low C_V in the Southeast Atlantic bracketed to the south where bloom detection was very low. The areas of low C_V were related to April SST with the 6°C isotherm associated with the northern boundary and 14°C the southern boundary.

To review, areas with high C_V tended to have short duration blooms associated with rapid increase and decline of chlorophyll concentrations and high bloom frequency, regardless of whether they occurred in spring or summer. Furthermore, these areas were also characterized as having a negative correlation between bloom start and duration, again regardless of whether the blooms were in spring or summer (Figures 5b & 6b). The areas with low C_V were associated with blooms peaking in summer, were often multi-season in duration, and were marked by having a slow increase and decline of chlorophyll concentrations. Furthermore, these areas did not show a correlation between bloom start and duration (Figure 6b).

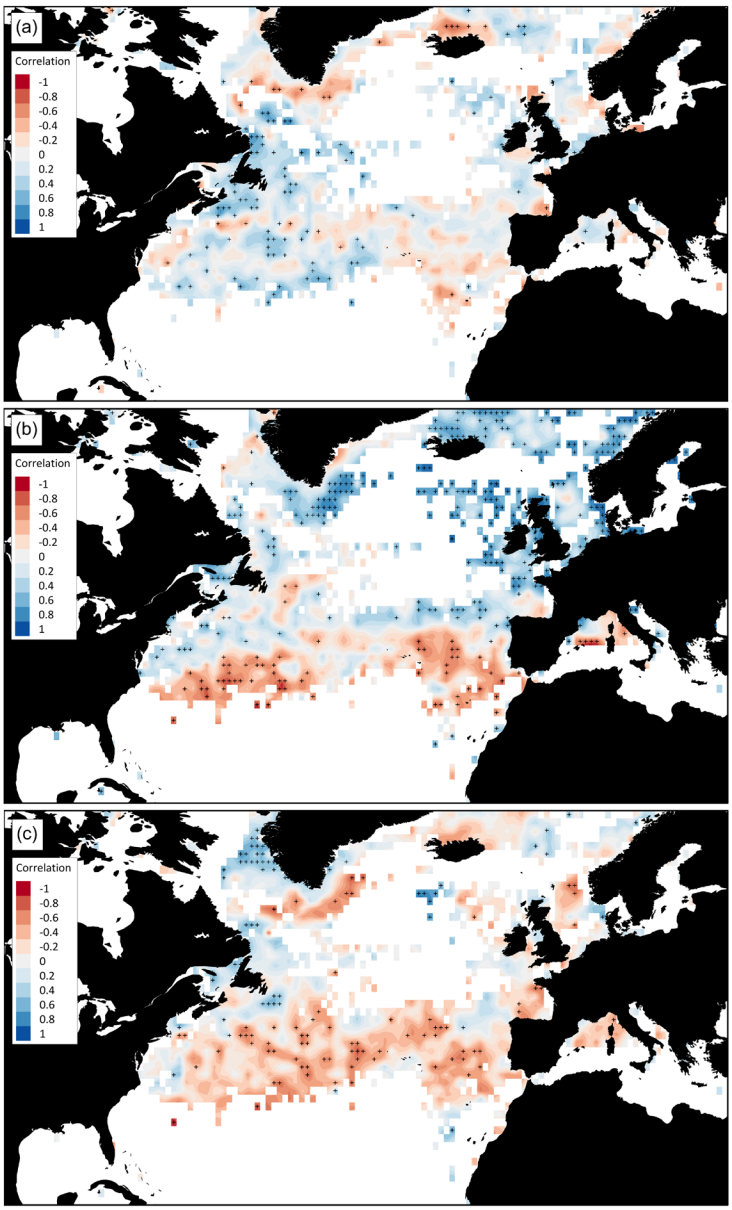

Figure 8

Correlation between bloom start day and thermal transition, temperature and the NAO.

Correlations between spring bloom start day and spring thermal transition day (a), sea surface temperature at the time of bloom start (b), and the North Atlantic Oscillation (c) for the period 1998–2014. Only grid locations with at least eight years with detected blooms were included; crosses mark locations with significant correlations ($\rho > 0.05$).

doi: 10.12952/journal.elementa.000099.f008

North Atlantic zooplankton

The abundances of small and large copepods showed contrasting latitudinal patterns. Small copepods were widely distributed across the North Atlantic at abundance levels generally above 100 m^{-3} (Figure 11a). In contrast, large copepods were in higher abundances at higher latitudes, generally in numbers above 10 m^{-3} and below 10 m^{-3} at lower latitudes (Figure 11b). The spatial abundance of large copepods was largely influenced by the distribution of *Calanus finmarchicus* (Fig. 12a), which is the dominant large zooplankton taxon in the North Atlantic. Neither pattern would appear to be related to the spatial distribution of bloom shape as indicated by the distribution of the shape parameter in the North Atlantic.

The areas of high abundance of the late stages of the four diapausing species of *Calanus* were associated with the boundaries between regions with low versus high bloom shape parameter. The abundance of *C. finmarchicus*, the most abundant species of this group, was associated with lower temperature regions around the North Atlantic and with the western boundary and part of the northern boundary between areas of low and high C_V (Figure 12a). The second most abundant species, *C. helgolandicus*, was found in warmer water temperatures and was associated with the eastern boundary between C_V areas and in the separation between two areas of low C_V in the eastern North Atlantic north and south of ~ 40°N (Figure 12b). The species *C. glacialis* and *C. hyperboreus* were found in low abundance in the CPR sampling area, but where they were found they were associated with the western boundary between areas of low and high C_V areas (Figures 12c, d). Collectively, these *Calanoid* taxa were associated with the areas of high C_V; and conversely, they were in low abundance in the areas having low C_V values.

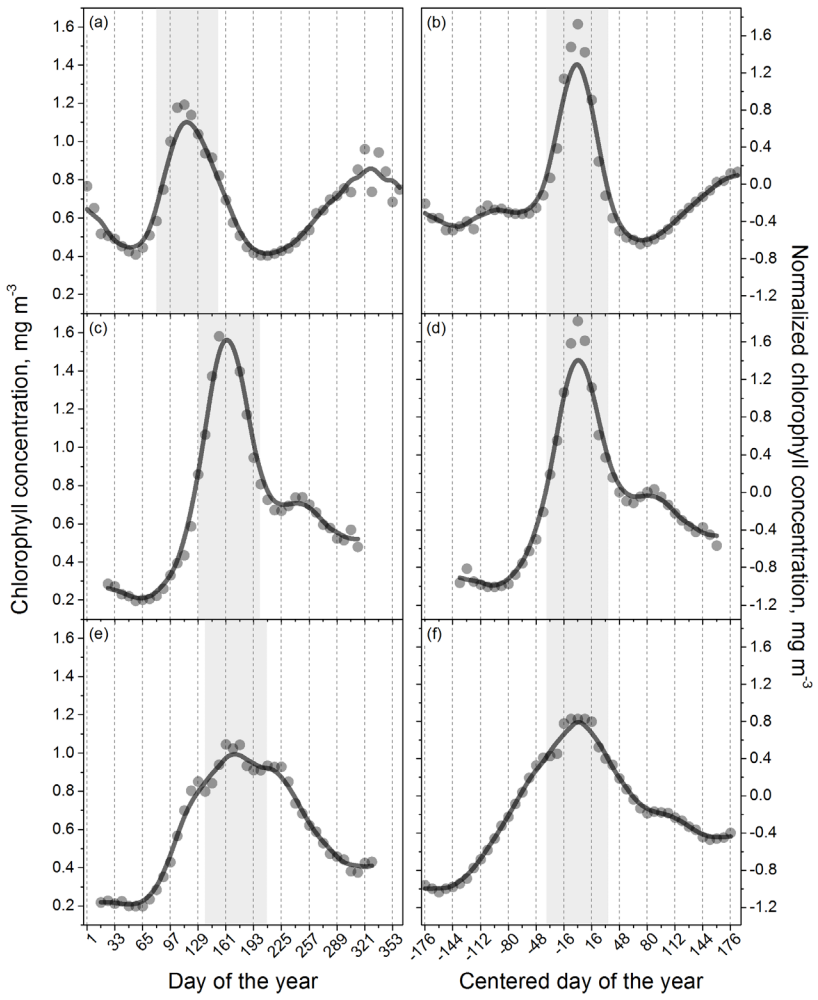

Figure 9

Index area annual chlorophyll concentrations.

Chlorophyll concentrations by day of the year and normalized chlorophyll concentration by centered day of the year for spring (a and b, respectively), summer high frequency (c and d, respectively), and summer low frequency (e and f, respectively) index areas (see Figure 1). In all plots, shaded grey areas mark a 9 8-day period duration limit for detected blooms.

doi: 10.12952/journal.elementa.000099.f009

Discussion

Our analysis is consistent with the key findings of other biogeographical studies of bloom patterns in the North Atlantic, and in addition identifies some rarely recognized features of internal bloom dynamics, in particular the relationships between bloom timing and duration. The first or principal bloom of the production cycle occurs in spring and continues into summer in the North Atlantic, with bloom start date ranging from March to June and later start dates tending to be farther north. We also identified annual production cycles that had a second bloom in the fall with start dates around September, which were contained in a latitudinal band between 40°N and 50°N. The area with high frequency of spring and summer blooms may be related to aspects of the general ocean circulation in the North Atlantic. The composite distribution of high frequency spring and summer blooms tracks the Gulf Stream bifurcation, and the North Atlantic Drift, Labrador, and Greenland Currents, whereas the area with low frequency blooms is mainly in the Iceland and Irminger Basins. Intuitively, the Icelandic and Irminger Basins would have more pronounced blooms due to their stronger seasonality of vertical mixing and associated nutrient supply supported by stronger winter convection suggested by deeper wintertime mixed layer depths (Monterey and Levitus, 1997). However, phytoplankton growth in these areas is also understood to be iron limited as suggested by both laboratory experiments and field observations (Nielsdottir et al., 2009; Ryan-Keogh et al., 2013). Consequently, phytoplankton cannot take up all the macronutrients replenished through winter mixing, leading to weak seasonal biomass fluctuations as shown in lower C_V areas. Moreover, areas with lower phytoplankton production are also less likely to provide suitable habitat for aggregations of zooplankton populations, which may exhibit top-down control that could potentially further shape the bloom pattern in the region as discussed below.

For areas and seasons where blooms occurred, we examined the effect of bloom timing on aspects of bloom development. The most consistent relationship we found was between bloom timing and duration: early developing blooms are longer lasting blooms. The correlations between bloom timing and either

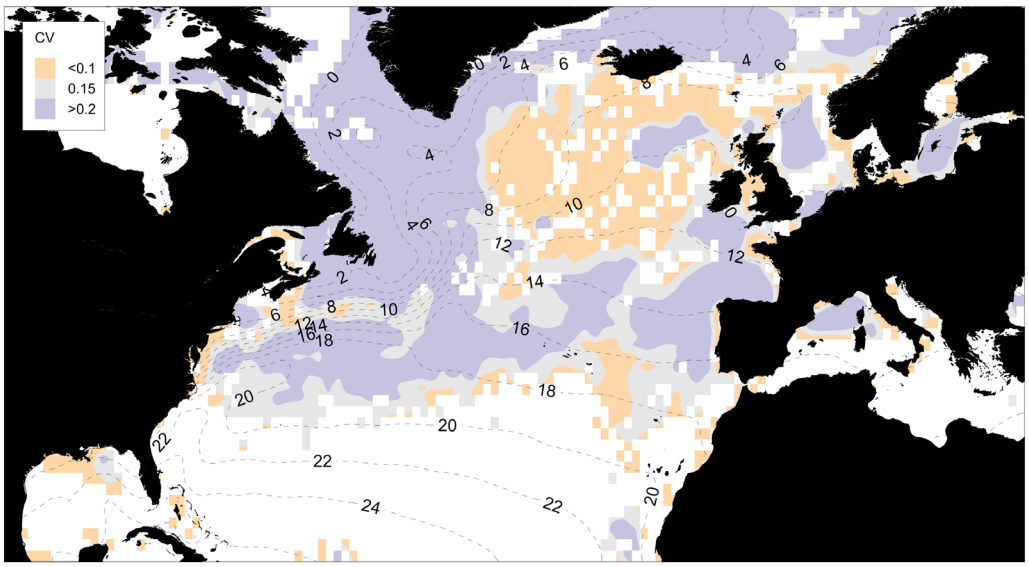

Figure 10

Bloom shape parameter and April SST.

Color filled contours represent the coefficient of variation (C_V) for chlorophyll concentrations over a period bracketing the annual maximum concentration ± five 8-day periods; only grid locations with at least eight years with detected spring or summer blooms were included for these contours. Labeled contours represent April SST (°C) for the period 1982–2014.

doi: 10.12952/journal.elementa.000099.f010

intensity or magnitude were weaker and must be viewed with lower confidence. With this caution in mind, it is worth noting that the correlation fields between bloom timing and magnitude tended to be negative, reflecting the influence of bloom duration on the calculation of magnitude. The correlation fields between bloom timing and intensity tended to be positive suggesting that later developing blooms tended to have higher chlorophyll concentrations.

It appears that different mechanisms are responsible for the onset and termination of the bloom. We hypothesize that the timing of the development of surface conditions that start the bloom may not be synchronized with conditions at depth, particularly the time at which grazers come out of diapause. Hence, early warming conditions in the surface may start the bloom, but the diapause schedule of grazers below the thermocline tends to occur with less variability than bloom initiation. This theme is explored below in greater detail as it relates to the distribution of copepods that diapause. We are also mindful of the potential role of nutrient limitation in determining the cessation and thus the persistence of blooms, which is characteristic of low latitude, oligotrophic waters dependent on nutrient upwelling (Polovina et al., 2008). However, at higher latitudes and the blooms represented in this study, nitrate seldom reaches limiting concentrations (Allen et al., 2005) and nutrient limitation is usually associated with silicate, which can limit the length of diatom blooms (Brzezinski et al., 1998). Silicate limitation could play a role in the shape of the decline of the bloom, as it often produces a transition from a highly productive diatom-dominated bloom phase to a more moderate bloom composed of a diverse phytoplankton assemblage (Egge and Aksnes, 1992; Sieracki et al., 1993). There is evidence that silicate limitation and grazing can interact to shape the termination of a bloom or the transition to a non-diatom community (Escaravage and Prins, 2002).

The North Atlantic can be divided into two regions related to the properties of the principal annual phytoplankton bloom and the putative role of grazing zooplankton in defining the development of blooms in these areas. Regions with short duration seasonal blooms are also associated with higher abundances of overwintered copepods that emerge and are found in the surface layers during spring. The presence of copepods that diapause alters the seasonality of grazing pressure, producing longer periods of more intensive copepod grazing, but also more intensive predation by copepods on microzooplankton. There is no known trigger or cue that consistently signals the descent into or the emergence from diapause, but the predominant theory is that the accumulation and metabolism of lipids play a major role (Johnson et al., 2008; Maps et al., 2014). Emergence from diapause often precedes the bloom maximum (Gislason et al., 2000; Johnson et al., 2008). This observation is consistent with the hypothesis that mesozooplankton predation of microzooplankton releases phytoplankton from grazing pressure, allowing the bloom to initiate (Behrenfeld and Boss, 2014). Regions with a higher abundance of diapausing copepod species correspond to regions where phytoplankton blooms are more rapid and pronounced, suggesting that top-down grazing and predation by copepods could have a role in shaping the bloom. However, we cannot rule out a bottom-up explanation. The dominance of copepods that diapause in certain regions could be a consequence of the pronounced phytoplankton blooms in those regions, as diapause is premised on the advantage it provides in highly seasonal conditions. In brief, punctuated blooms are followed by extended periods of low prey availability for large copepods, giving an advantage to those copepod species that can accumulate lipids and survive periods without food. In order to distinguish between these possible explanations, we require more detailed information on the proportion of copepod diets *in situ* that are comprised of phytoplankton versus microzooplankton, as well as *in situ* grazing rates.

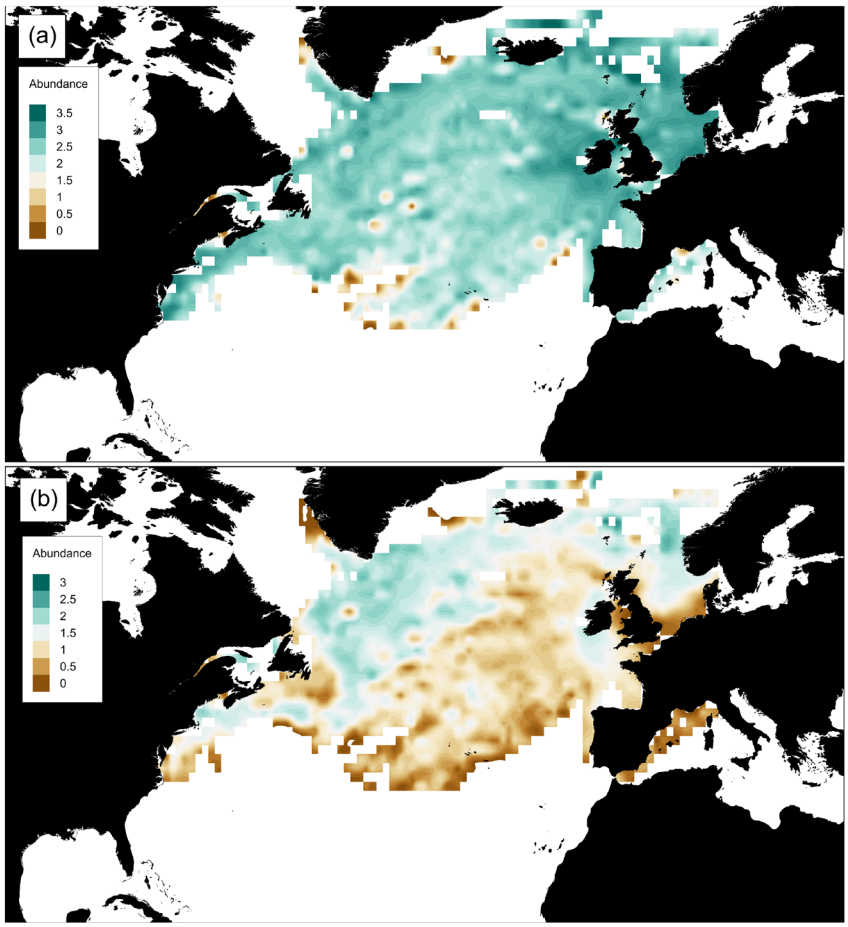

Figure 11

Small and large zooplankton abundance distribution.

Abundance (log m^{-3}) of small (a) and large (b) copepods in the North Atlantic over the time period 1958–2013.

doi: 10.12952/journal.elementa.000099.f011

Diapause is often a prominent feature of modeling studies that focus on copepods (Aita et al., 2007; Miller et al., 1998; Record et al., 2013; Varpe et al., 2007; Zakardjian et al., 2003), but global and biogeochemical ocean models do not include diapause. Grazers have been included in predictive models of blooms for many years (Riley, 1946). In a typical biogeochemical model, however, mesozooplankton grazing is an increasing function of mesozooplankton abundance, a formulation that is at odds with the reality of many seasonal oceans where the biomass of large zooplankton is at or near its highest value during diapause at a time when the grazing rate is very low. If diapause does indeed play an important role in the development of phytoplankton blooms in these regions, an explicit incorporation of diapause will be necessary to reliably reproduce bloom dynamics, and by implication carbon cycling, in seasonal oceans.

The variation in bloom dynamics observed in the North Atlantic in this study has implications for efforts to estimate regional patterns of carbon flux (Henson et al., 2012). There is generally a correlation between bloom timing and duration, with earlier blooms tending to produce longer-lasting blooms. Extended blooms imply that grazing pressure may be relatively weak in segments of the basin. The resulting effect on the efficiency of carbon export is difficult to predict: reduced grazing implies fewer fecal pellets which are an efficient vector for transporting carbon to the mesopelagic (Abramson et al., 2010; Herndl and Reinthaler, 2013); on the other hand, reduced grazing may allow more phytoplankton to accumulate in the euphotic zone, presumably enhancing aggregation and therefore export of phytodetritus (Turner, 2015). An earlier bloom may facilitate the development of more intense blooms, which might go ungrazed and intensify export from the euphotic zone (Kahru et al., 2011). Bloom duration may be a useful additional metric to understand how spatial variability in export efficiency arises.

Initiation of the spring bloom appears to be related to spring thermal conditions and the North Atlantic Oscillation on a regional basis. The timing of the thermal transition may be associated with the water column changes central to the critical depth (Sverdrup, 1953) and Dilution–Recoupling (Behrenfeld, 2010) hypotheses of bloom initiation. Alternatively, changes in critical depth and stratification can also be affected by salinity and sea ice dynamics, as well as seasonal changes in light availability, which can also cause the critical depth to shoal (Capotondi et al., 2012). The influence of the spring thermal transition on bloom initiation is less likely to be related to the critical turbulence hypothesis, which would be more likely related to changes in wind

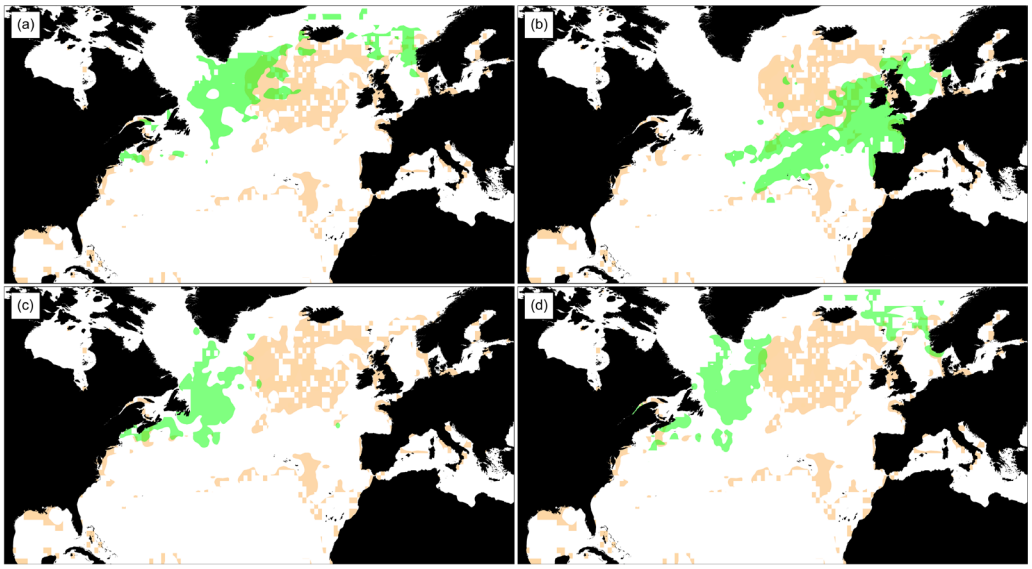

Figure 12

Regions of bloom shape parameter minima and high abundance of copepods that diapause.

Regions of high abundance of *Calanus finmarchicus* (a, > 1.7 log m^{-3}), *C. helgolandicus* (b, > 0.5 log m^{-3}), *C. glacialis* (c, > 0.05 log m^{-3}), *C. hyperboreus* (d, > 0.05 log m^{-3}), overlaid on area of low C_V (< 0.1) bloom shape parameter from Figure 10, shown as beige in all panels.

doi: 10.12952/journal.elementa.000099.f012

stress and/or heat flux (Huisman et al., 1999; Taylor and Ferrari, 2011). Moreover, active turbulence in the ocean is highly variable in both space and time (Franks, 2014). The positive correlation field between thermal transition and bloom start day was relatively weak, but strongest in areas where the spring bloom was most consistently detected. In areas where bloom start was independent of transition day, SST was either positively or negatively correlated with bloom start day. In northern latitudes, the positive correlation suggests bloom initiation is independent of temperature and related to other factors controlling water column stability. The areas of negative correlation between SST and bloom start day suggest accelerated warming can influence the start of the bloom. The NAO has been shown to affect trends in lower trophic levels in the North Atlantic, including the composition of phytoplankton and zooplankton communities (Henson et al., 2012; Irigoien et al., 2000; Piontkovski et al., 2006; Zhai et al., 2013). We find that the NAO is positively and negatively correlated to bloom timing in different regions. The areas with positive and negative NAO correlation were also areas where we observed little correlation between thermal transition and bloom start, suggesting that physical forcing other than local temperature may be at work (e.g., wind, nutrient concentration). However, in the Northwest Atlantic the opposite sign may be a result of advective processes and the lagged response of the NAO on water temperature in lower latitude waters like the Gulf of Maine (Xu et al., 2015). The delineation between areas where bloom start is related to thermal transition or the NAO were clearer in northern latitudes, whereas correlations with thermal transition and NAO are interspersed in southern latitudes, suggesting bloom start was defined by local conditions instead of basin-scale forcing associated with the NAO.

Recruitment success of marine fish depends on progeny being spawned into an environment suitable for feeding, rapid growth, and development that ensures high survival rates. Seasonal and annual variability of the phenology of prey and larval fish can lead to match or mismatch between the timing of peak abundance of either. Zooplankton feeding and growth is often associated with years with early spring blooms and optimal temperatures, which can lead to optimal feeding conditions for larval fish. The early access to prey leads to a prolonged season where high growth rates can be achieved and higher cumulative numbers of larval fish that survive the critical early life stages (Kristiansen et al., 2011). One aspect of the match-mismatch theory (Cushing, 1996; Hjort, 1914) that is often not considered fully, is the importance of the spatial variability in match-mismatch (Durant et al., 2007). This match-mismatch in the timing of the spring bloom and fish spawning has been seen in a range of fish species (Malick et al., 2015; Trzcinski et al., 2013; Visser et al., 2011), and in some cases the timing of the fall bloom appears to be the critical factor (Leaf and Friedland, 2014). Linkages have also been developed between the size of the spring bloom and fish stock productivity (Chittenden et al., 2010; Schweigert et al., 2013). By utilizing satellite observations we can identify patterns in seasonal blooms and more effectively evaluate the linkages between primary production and the annual and spatial variability in recruitment and fisheries productivity.

In conclusion, this study demonstrates that interannual variations in bloom onset timing influence the subsequent development of phytoplankton blooms, with a particularly strong effect on bloom duration. Early blooms tend to be longer lasting, possibly due to reduced grazing pressure. Grazing pressure by copepods that diapause also appears to be linked to the shape of the bloom, with longer lasting, multi-season blooms occurring in areas where these copepod taxa are largely absent. These results have implications for both carbon export of primary production to the benthos and the linkage between primary productivity and fish production.

References

Abramson L, Lee C, Liu ZF, Wakeham SG, Szlosek J. 2010. Exchange between suspended and sinking particles in the northwest Mediterranean as inferred from the organic composition of *in situ* pump and sediment trap samples. *Limnol Oceanogr* **55**(2): 725–739.

Aita MN, Yamanaka Y, Kishi MJ. 2007. Interdecadal variation of the lower trophic ecosystem in the northern Pacific between 1948 and 2002, in a 3-D implementation of the NEMURO model. *Ecol Mod* **202**(1–2): 81–94.

Allen JT, Brown L, Sanders R, Moore CM, Mustard A, et al. 2005. Diatom carbon export enhanced by silicate upwelling in the northeast Atlantic. *Nature* **437**(7059): 728–732.

Banse K. 2013. Reflections about chance in my career, and on the top-down regulated world. *Annu Rev Mar Sci* **5**: 1–19.

Behrenfeld MJ. 2010. Abandoning Sverdrup's Critical Depth Hypothesis on phytoplankton blooms. *Ecology* **91**(4): 977–989.

Behrenfeld MJ, Boss ES. 2014. Resurrecting the ecological underpinnings of ocean plankton blooms. *Annu Rev Mar Sci* **6**: 167–208.

Bidle KD, Falkowski PG. 2004. Cell death in planktonic, photosynthetic microorganisms. *Nat Rev Microbiol* **2**(8): 643–655.

Bidle KD, Vardi A. 2011. A chemical arms race at sea mediates algal host-virus interactions. *Curr Opin Microbiol* **14**(4): 449–457.

Blondeau-Patissier D, Gower JFR, Dekker AG, Phinn SR, Brando VE. 2014. A review of ocean color remote sensing methods and statistical techniques for the detection, mapping and analysis of phytoplankton blooms in coastal and open oceans. *Prog Oceanogr* **123**: 123–144.

Brody SR, Lozier MS, Dunne JP. 2013. A comparison of methods to determine phytoplankton bloom initiation. *J Geophys Res-Oceans* **118**(5): 2345–2357.

Brzezinski MA, Villareal TA, Lipschultz F. 1998. Silica production and the contribution of diatoms to new and primary production in the central North Pacific. *Mar Ecol: Prog Ser* **167**: 89–104.

Capotondi A, Alexander MA, Bond NA, Curchitser EN, Scott JD. 2012. Enhanced upper ocean stratification with climate change in the CMIP3 models. *J Geophys Res-Oceans* **117**. doi: 10.1029/2011JC007409.

Chen B, Zheng L, Huang B, Song S, Liu H. 2013. Seasonal and spatial comparisons of phytoplankton growth and mortality rates due to microzooplankton grazing in the northern South China Sea. *Biogeosciences* **10**(4): 2775–2785.

Chiswell SM, Calil PHR, Boyd PW. 2015. Spring blooms and annual cycles of phytoplankton: A unified perspective. *J Plankton Res* **37**(3): 500–508.

Chittenden CM, Jensen JLA, Ewart D, Anderson S, Balfry S, et al. 2010. Recent salmon declines: A result of lost feeding opportunities due to bad timing? *PLOS One* **5**(8). doi: 10.1371/journal.pone.0012423.

Cushing DH. 1996. Towards a science of recruitment in fish populations, in, Kinne O, ed., *Excellence in Ecology*. Vol. **7**. Oldendorf, Germany: Ecology Institute Nordbunte.

D'Ortenzio F, Antoine D, Martinez E, d'Alcala MR. 2012. Phenological changes of oceanic phytoplankton in the 1980s and 2000s as revealed by remotely sensed ocean-color observations. *Global Biogeochem Cy* **26**. doi: 10.1029/2011GB004269.

Durant JM, Hjermann DO, Ottersen G, Stenseth NC. 2007. Climate and the match or mismatch between predator requirements and resource availability. *Climate Res* **33**(3): 271–283.

Egge JK, Aksnes DL. 1992. Silicate as regulating nutrient in phytoplankton competition. *Mar Ecol: Prog Ser* **83**(2–3): 281–289.

Escaravage V, Prins TC. 2002. Silicate availability, vertical mixing and grazing control of phytoplankton blooms in mesocosms. *Hydrobiologia* **484**(1–3): 33–48.

Follows M, Dutkiewicz S. 2002. Meteorological modulation of the North Atlantic spring bloom. *Deep-Sea Res Pt II* **49**(1–3): 321–344.

Franks PJS. 2014. Has Sverdrup's critical depth hypothesis been tested? Mixed layers vs. turbulent layers. *ICES J Mar Sci*. **72**(6): 1897–1907. doi: 10.1093/icesjms/fsu175.

Friedland KD, Hare JA, Wood GB, Col LA, Buckley LJ, et al. 2008. Does the fall phytoplankton bloom control recruitment of Georges Bank haddock, *Melanogrammus aeglefinus*, through parental condition? *Can J Fish Aquat Sci* **65**(6): 1076–1086.

Friedland KD, Hare JA, Wood GB, Col LA, Buckley LJ, et al. 2009. Reply to the comment by Payne et al. on "Does the fall phytoplankton bloom control recruitment of Georges Bank haddock, *Melanogrammus aeglefinus*, through parental condition?" *Can J Fish Aquat Sci* **65**(5): 873–877.

Friedland KD, Leaf RT, Kane J, Tommasi D, Asch RG, et al. 2015. Spring bloom dynamics and zooplankton biomass response on the US Northeast Continental Shelf. *Cont Shelf Res* **102**(0): 47–61.

Friedland KD, Todd CD. 2012. Changes in Northwest Atlantic Arctic and Subarctic conditions and the growth response of Atlantic salmon. *Polar Biol* **35**(4): 593–609.

Gislason A, Astthorsson OS, Petursdottir H, Gudfinnsson H, Bodvarsdottir AR. 2000. Life cycle of *Calanus finmarchicus* south of Iceland in relation to hydrography and chlorophyll a. *ICES J Mar Sci* **57**(6): 1619–1627.

Hélaouët P, Beaugrand G, Reygondeau G. 2016. Reliability of spatial and temporal patterns of *C. finmarchicus* inferred from the CPR survey. *J Mar Syst* **153**: 18–24.

Henson S, Lampitt R, Johns D. 2012. Variability in phytoplankton community structure in response to the North Atlantic Oscillation and implications for organic carbon flux. *Limnol Oceanogr* **57**(6): 1591–1601.

Henson SA, Dunne JP, Sarmiento JL. 2009. Decadal variability in North Atlantic phytoplankton blooms. *J Geophys Res-Oceans* **114**. doi: 10.1029/2008jc005139.

Henson SA, Thomas AC. 2007. Interannual variability in timing of bloom initiation in the California Current System. *J Geophys Res-Oceans* **112**(C8). doi: 10.1029/2006jc003960.

Herndl GJ, Reinthaler T. 2013. Microbial control of the dark end of the biological pump. *Nat Geosci* **6**(9): 718–724.

Hjort J. 1914. Fluctuations in the great fisheries of northern Europe, viewed in the light of biological research. *Rapp P-V Reun - Cons Int Explor Mer* **20**: 1–228.

Huisman J, van Oostveen P, Weissing FJ. 1999. Critical depth and critical turbulence: Two different mechanisms for the development of phytoplankton blooms. *Limnol Oceanogr* **44**(7): 1781–1787.

Hurrell JW, Kushnir Y, Visbeck M. 2001. Climate - The North Atlantic Oscillation. *Science* **291**(5504): 603–605.

Irigoien X, Harris RP, Head RN, Harbour D. 2000. North Atlantic Oscillation and spring bloom phytoplankton composition in the English Channel. *J Plankton Res* **22**(12): 2367–2371.
Johnson CL, Leising AW, Runge JA, Head EJH, Pepin P, et al. 2008. Characteristics of *Calanus finmarchicus* dormancy patterns in the Northwest Atlantic. *ICES J Mar Sci* **65**(3): 339–350.
Kahru M, Brotas V, Manzano-Sarabia M, Mitchell BG. 2011. Are phytoplankton blooms occurring earlier in the Arctic? *Global Change Biol* **17**(4): 1733–1739.
Kiørboe T, Møhlenberg F, Riisgård HU. 1985. *In situ* feeding rates of plantonic copepods: A comparison of four methods. *J Exp Mar Biol Ecol* **88**(1): 67–81.
Kristiansen T, Drinkwater KF, Lough RG, Sundby S. 2011. Recruitment variability in North Atlantic cod and match-mismatch dynamics. *PLOS One* **6**(3): e17456.
Lacour L, Claustre H, Prieur L, D'Ortenzio F. 2015. Phytoplankton biomass cycles in the North Atlantic subpolar gyre: A similar mechanism for two different blooms in the Labrador Sea. *Geophys Res Lett* **42**(13): 5403–5410.
Landry MR, Calbet A. 2004. Microzooplankton production in the oceans. *ICES J Mar Sci* **61**(4): 501–507.
Leaf RT, Friedland KD. 2014. Autumn bloom phenology and magnitude influence haddock recruitment on Georges Bank. *ICES J Mar Sci* **71**: 2017–2015.
Malick MJ, Cox SP, Mueter FJ, Peterman RM. 2015. Linking phytoplankton phenology to salmon productivity along a north-south gradient in the Northeast Pacific Ocean. *Can J Fish Aquat Sci* **72**(5): 697–708.
Maps F, Record NR, Pershing AJ. 2014. A metabolic approach to dormancy in pelagic copepods helps explaining inter- and intra-specific variability in life-history strategies. *J Plankton Res* **36**(1): 18–30.
Maritorena S, d'Andon OHF, Mangin A, Siegel DA. 2010. Merged satellite ocean color data products using a bio-optical model: Characteristics, benefits and issues. *Remote Sens Env* **114**(8): 1791–1804.
Martinez E, Antoine D, D'Ortenzio F, Montegut CD. 2011. Phytoplankton spring and fall blooms in the North Atlantic in the 1980s and 2000s. *J Geophys Res-Oceans* **116**. doi: 10.1029/2006jc003960.
Miller CB, Lynch DR, Carlotti F, Gentleman W, Lewis CVW. 1998. Coupling of an individual-based population dynamic model of *Calanus finmarchicus* to a circulation model for the Georges Bank region. *Fish Oceanogr* **7**(3–4): 219–234.
Monterey G, Levitus S. 1997. Seasonal Variability of Mixed Layer Depth for the World Ocean. *NOAA Atlas NESDIS 14*. Washington, D.C.: U.S. Gov. Printing Office: 96 pp.
Nielsdottir MC, Moore CM, Sanders R, Hinz DJ, Achterberg EP. 2009. Iron limitation of the postbloom phytoplankton communities in the Iceland Basin. *Global Biogeochem Cy* **23**. doi: 10.1029/2008gb003410.
Piontkovski SA, O'Brien TD, Umani SF, Krupa EG, Stuge TS, et al. 2006. Zooplankton and the North Atlantic Oscillation: A basin-scale analysis. *J Plankton Res* **28**(11): 1039–1046.
Polovina JJ, Howell EA, Abecassis M. 2008. Ocean's least productive waters are expanding. *Geophys Res Lett* **35**(3). doi: 10.1029/2007gl031745.
Racault MF, Le Quere C, Buitenhuis E, Sathyendranath S, Platt T. 2012. Phytoplankton phenology in the global ocean. *Ecol Indicators* **14**(1): 152–163.
Record NR, Pershing AJ, Maps F. 2013. Emergent copepod communities in an adaptive trait-structured model. *Ecol Mod* **260**: 11–24.
Reynolds RW, Smith TM, Liu C, Chelton DB, Casey KS, et al. 2007. Daily high-resolution-blended analyses for sea surface temperature. *J Clim* **20**(22): 5473–5496.
Richardson AJ, Walne AW, John AWG, Jonas TD, Lindley JA, et al. 2006. Using continuous plankton recorder data. *Prog Oceanogr* **68**(1): 27–74.
Riley GA. 1946. Factors controlling phytoplankton populations on Georges Bank. *J Mar Res* **6**: 54–73.
Rodionov SN. 2004. A sequential algorithm for testing climate regime shifts. *Geophys Res Lett* **31**(9). doi: 10.1029/2004gl019448.
Rodionov SN. 2006. Use of prewhitening in climate regime shift detection. *Geophys Res Lett* **33**(12). doi: 10.1029/2006gl025904.
Ryan-Keogh TJ, Macey AI, Nielsdottir MC, Lucas MI, Steigenberger SS, et al. 2013. Spatial and temporal development of phytoplankton iron stress in relation to bloom dynamics in the high-latitude North Atlantic Ocean. *Limnol Oceanogr* **58**(2): 533–545.
Sapiano MRP, Brown CW, Uz SS, Vargas M. 2012. Establishing a global climatology of marine phytoplankton phenological characteristics. *J Geophys Res-Oceans* **117**. doi: 10.1029/2012jc007958.
Schweigert JF, Thompson M, Fort C, Hay DE, Therriault TW, et al. 2013. Factors linking Pacific herring (*Clupea pallasi*) productivity and the spring plankton bloom in the Strait of Georgia, British Columbia, Canada. *Prog Oceanogr* **115**: 103–110.
Sieracki ME, Verity PG, Stoecker DK. 1993. Plankton community response to sequential silicate and nitrate depletion during the 1989 North-Atlantic spring bloom. *Deep-Sea Res Pt II* **40**(1–2): 213–225.
Song HJ, Ji RB, Stock C, Kearney K, Wang ZL. 2011. Interannual variability in phytoplankton blooms and plankton productivity over the Nova Scotian Shelf and in the Gulf of Maine. *Mar Ecol: Prog Ser* **426**: 105–133.
Suttle CA, Chan AM, Cottrell MT. 1990. Infection of phytoplankton by viruses and reduction of primary productivity. *Nature* **347**(6292): 467–469.
Sverdrup HU. 1953. On conditions for the vernal blooming of phytoplankton. *J Cons Explor Mer* **18**: 287–295.
Taboada FG, Anadon R. 2014. Seasonality of North Atlantic phytoplankton from space: Impact of environmental forcing on a changing phenology (1998–2012). *Global Change Biol* **20**(3): 698–712.
Taylor JR, Ferrari R. 2011. Shutdown of turbulent convection as a new criterion for the onset of spring phytoplankton blooms. *Limnol Oceanogr* **56**(6): 2293–2307.
Trzcinski MK, Devred E, Platt T, Sathyendranath S. 2013. Variation in ocean colour may help predict cod and haddock recruitment. *Mar Ecol: Prog Ser* **491**: 187–197.
Turner JT. 2015. Zooplankton fecal pellets, marine snow, phytodetritus and the ocean's biological pump. *Prog Oceanogr* **130**: 205–248.
Ueyama R, Monger BC. 2005. Wind-induced modulation of seasonal phytoplankton blooms in the North Atlantic derived from satellite observations. *Limnol Oceanogr* **50**(6): 1820–1829.

Vargas M, Brown CW, Sapiano MRP. 2009. Phenology of marine phytoplankton from satellite ocean color measurements. *Geophys Res Lett* **36**. doi: 10.1029/2008gl036006.
Varpe O, Jorgensen C, Tarling GA, Fiksen O. 2007. Early is better: Seasonal egg fitness and timing of reproduction in a zooplankton life-history model. *Oikos* **116**(8): 1331–1342.
Verity PG, Stoecker DK, Sieracki ME, Nelson JR. 1993. Grazing, growth and mortality of microzooplankton during the 1989 North Atlantic spring bloom at 47°N, 18°W. *Deep-Sea Res Pt I* **40**(9): 1793–1814.
Visser F, Hartman KL, Pierce GJ, Valavanis VD, Huisman J. 2011. Timing of migratory baleen whales at the Azores in relation to the North Atlantic spring bloom. *Mar Ecol: Prog Ser* **440**: 267–279.
Wilson RJ, Speirs DC, Heath MR. 2015. On the surprising lack of differences between two congeneric calanoid copepod species, *Calanus finmarchicus* and *C. helgolandicus*. *Prog Oceanogr* **134**: 413–431.
Xu H, Kim H-M, Nye JA, Hameed S. 2015. Impacts of the North Atlantic Oscillation on sea surface temperature on the Northeast US Continental Shelf. *Cont Shelf Res* **105**(0): 60–66.
Zakardjian BA, Sheng JY, Runge JA, McLaren I, Plourde S, et al. 2003. Effects of temperature and circulation on the population dynamics of *Calanus finmarchicus* in the Gulf of St. Lawrence and Scotian Shelf: Study with a coupled, three-dimensional hydrodynamic, stage-based life history model. *J Geophys Res-Oceans* **108**(C11). doi: 10.1029/2002jc001410.
Zhai L, Platt T, Tang C, Sathyendranath S, Walne A. 2013. The response of phytoplankton to climate variability associated with the North Atlantic Oscillation. *Deep-Sea Res Pt II* **93**: 159–168.

Contributions

- Contributed to conception and design: KDF, NRR, DGJ
- Contributed to acquisition of data: KDF, RTL, DGJ
- Contributed to analysis and interpretation of data: KDF, NRR, SH, DGJ, RGA, RJ
- Drafted and/or revised the article: KDF, NRR, RGA, TK, VSS, KFD, SH, RTL, REM, DGJ, SIL, SSH, JAN, MAA, RJ
- Approved the submitted version for publication: KDF, NRR, RGA, TK, VSS, KFD, SH, RTL, REM, DGJ, SIL, SSH, JAN, MAA, RJ

Acknowledgments

The authors wish to thank the Norwegian Research Council funded NUCCME (Norway-United States Climate Change and Marine Ecosystems) Project and the Nordic Council funded CLIFFIMA (Climate Impacts on Fish and the Fisheries Industry and Management in the Nordic Seas) Network for sponsoring the Workshop in Ulvik, Norway, at which this paper was begun and for covering publication costs. We also thank the Sir Alister Hardy Foundation for Ocean Science (SAHFOS) for the provision of zooplankton data.

Funding information

RA was funded by Nippon Foundation-UBC Nereus Program.

Competing interests

None of the authors declare a competing interest for the work reported in this publication.

Data accessibility statement

All data will be publically available.